ERCOFTAC Design Optimization: Methods & Applications

International Conference & Advanced Course
Athens, Greece, March 31- April 2, 2004

Conference Proceedings
Editors: K.C. Giannakoglou (NTUA), W. Haase (EADS-M)

ERCODO2004_215

Adjoint-Based Shape Optimization for Natural Laminar Flow Design

O. Amoignon
J.O. Pralits
A. Hanifi
M. Berggren
D. S. Henningson

[(1)(4)] Uppsala University, SWEDEN
[(2)] Salermo University, ITALY
[(2)(3)(4)(5)] FOI, SWEDEN
[(5)] KTH, SWEDEN

Design Optimization International Conference,
March 31- April 2 2004, Athens, Greece,

ADJOINT-BASED SHAPE OPTIMIZATION FOR NATURAL LAMINAR FLOW DESIGN

Olivier Amoignon[*], Jan O. Pralits[†‡], Ardeshir Hanifi[‡], Martin Berggren[*‡], Dan S. Henningson[‡§]

[*]Uppsala University, Department of Information Technology, SE-751 05 Uppsala, Sweden,
[†]Salerno University, Department of Mechanical Engineering, 84084 Fisciano, Italy,
[‡]FOI, Aeronautics Division, FFA, SE-172 90, Stockholm, Sweden,
[§]KTH, Department of Mechanics, SE-100 44 Stockholm, Sweden,

Key words: Adjoint equations, boundary layer equations, Euler equations, natural laminar flow, parabolized stability equations, transition.

Abstract. *Gradient-based shape optimization of an airfoil is performed with respect to the location of the laminar-turbulent transition in the boundary layer. The shape gradients are efficiently computed based on the solutions of the adjoint equations of the Euler, boundary-layer and stability equations. Results show a reduction of the total amplification of a large number of disturbances, which is assumed to represent a delay of the transition in the boundary layer. As delay of the transition implies reduction of the viscous drag, the present method enables shape optimization to perform viscous drag reduction.*

1 Introduction

The reduction of both the pressure and viscous drag of high-speed vehicles is a challenging task. The use of laminar flow control techniques aims at delaying the laminar-turbulent transition which is known to reduce the viscous drag coefficient (see [17] for an overview). CFD-based design optimization has proved to be successful in reducing the pressure drag at transonic flow regime (see for example [15]). However, optimal shape design aiming at total drag minimization has relied on fixing the point of laminar-turbulent transition or on the assumption that the flow is fully turbulent as in [21]. In [2], CFD calculation is complemented by an analysis of the growth rate of disturbances superimposed on the laminar flow in the boundary layer, and, for the first time, the shape sensitivities of the energy of disturbances are calculated by an adjoint approach involving the Euler, boundary-layer and stability equations. With this approach, the shape of an airfoil can be optimized with respect to the energy of disturbances for the purpose of delaying laminar-turbulent transition.

1.1 Active control of transition and CFD-based optimization

Laminar-turbulent transition in the boundary layer on aircraft wings is usually caused by breakdown of small disturbances that grow as they propagate downstream. The amplification of these disturbances can be analyzed using linear stability theory, in which it is assumed that disturbances with infinitesimal amplitude are superimposed on the laminar mean flow. The

growth rate of the disturbances can then be used to predict the transition location using the so called e^N method, [32], [29], [4].

Linear stability analysis and the use of adjoint equations has allowed to efficiently search for optimal (active) control of the transition, [25], [26].

In parallel to the use of adjoint equations in control optimization, research teams have developed adjoint codes for the design of aircrafts with lower drag, [3], [6] [8], [10], [11], [16], [20], [27], [30], [31].

1.2 Optimal NLF design

The design of shapes such that the laminar portion is increased is denoted as Natural Laminar Flow (NLF) design, [12], [19]. However, previous attempts have been limited to inverse design approaches or non-gradient optimization, with a few parameters of design in the last case.

In the present contribution, CFD calculation is used to analyze the growth rate of disturbances superimposed on the laminar flow in the boundary layer:

- The solution of the Euler equations provides a pressure distribution on the surface of the geometry defined by the design parameters.
- The viscous mean flow is obtained by solving the boundary layer equations for compressible flows over infinite swept wings, given the pressure distribution and the geometry.
- The linear stability equations are solved given the viscous mean flow and the geometry, providing the amplitude and phase of a specific disturbance.

With this approach, the shape, here an airfoil, can be optimized with respect to the energy of disturbances for the purpose of delaying laminar-turbulent transition.

The present work contributes to the field of optimal NLF design as the solutions of the adjoint equations of the three states above are combined to obtain the shape derivative of the energy of a disturbance, enabling to carry large scale optimization.

The presentation that follows gives a brief description of the state equation systems and of the objective function. The systems of adjoint equations can be found in the references [24] for the adjoint of the stability equations, [23] and [25] for the adjoint of the boundary layer equations, and [1] for the discrete adjoint of the Euler equations.

The parameterization of the shape allows to define non trivial feasible sets by including constraints (fixed parts of the wing, fixed volume) in a general manner. The approach is shortly explained here.

The formulated optimization problem, applied on the airfoil RAE 2822, succeeds to simultaneously reduce the pressure drag and to reduce the total amplification of a large number of disturbances at constant lift and pitch moment coefficients, and within the set of feasible designs mentioned above.

2 State equations and objective function

2.1 Inviscid flow

The Euler equations express the conservation of mass, the conservation of momentum, and the conservation of energy, written here in integral form for an arbitrary fixed region V with

boundary ∂V,

$$\frac{\partial}{\partial t}\int_V \rho \mathrm{dX} + \int_{\partial V} \rho \mathbf{u}\cdot\hat{\mathbf{n}}\mathrm{dS} = 0\,, \tag{1}$$

$$\frac{\partial}{\partial t}\int_V \rho \mathbf{u}\mathrm{dX} + \int_{\partial V} \rho \mathbf{u}\,\mathbf{u}\cdot\hat{\mathbf{n}}\mathrm{dS} + \int_{\partial V} p\hat{\mathbf{n}}\mathrm{dS} = \mathbf{0}\,, \tag{2}$$

$$\frac{\partial}{\partial t}\int_V E\mathrm{dX} + \int_{\partial V} \mathbf{u}E\cdot\hat{\mathbf{n}}\mathrm{dS} + \int_{\partial V} p\mathbf{u}\cdot\hat{\mathbf{n}}\mathrm{dS} = 0\,, \tag{3}$$

where $\hat{\mathbf{n}}$ is the unit outward-oriented normal on ∂V, E is the total energy per unit volume, which for an ideal fluid is related to the temperature and the velocity. The law of perfect gas closes the system by relating pressure, density and temperature. The program Edge [9] solves equation 1, together with boundary conditions, using a node-centred and edge-based finite-volume approximation. This type of discretization, based on a dual grid, can be found in [5].

2.2 Viscous flow

The flow field considered here is the boundary layer on a swept wing with infinite span, which is obtained by solving the mass, momentum, and energy conservation equations for a viscous compressible fluid. The equations are written in an orthogonal curvilinear coordinate system. A characteristic length of an element, assuming an infinite swept wing, is defined by $ds^2 = (h_1 dx^1)^2 + (dx^2)^2 + (dx^3)^2$. The total flow field, Q_{tot} is decomposed into a mean, $\bar{Q}$, and a perturbation part, $\tilde{Q}$, as

$$Q_{tot}(x^1, x^2, x^3, t) = \bar{Q}(x^1, x^3) + \tilde{Q}(x^1, x^2, x^3, t)$$

where $\bar{Q}$ is one of the mean variables $[\bar{U}, \bar{V}, \bar{W}, \bar{P}, \bar{T}, \bar{\rho}]$ and $\widetilde{Q}$ is the corresponding disturbance variable among $[\tilde{U}, \tilde{V}, \tilde{W}, \tilde{P}, \tilde{T}, \tilde{\rho}]$. The equations are derived for a quasi three-dimensional mean flow with zero variation in the spanwise direction. The evolution of convectively unstable disturbances is analyzed in the framework of the nonlocal stability theory. All flow and material quantities are made dimensionless with the corresponding reference flow quantities at a fixed streamwise position x_0, except the pressure, which is made dimensionless with twice the corresponding dynamic pressure. The reference length scale is taken as $l_0 = (\bar{\nu}_0 x_0/\bar{u}_0)^{\frac{1}{2}}$, and the Reynolds and Mach number are defined as $Re = l_0\bar{u}_0/\bar{\nu}_0$ and $M = \bar{u}_0/(\mathcal{R}\gamma\bar{T}_0)^{\frac{1}{2}}$ respectively.

2.2.1 Mean-flow equations

The dimensionless boundary-layer equations modelling the steady viscous compressible mean flow on a swept wing with infinite span written in primitive variable form are given as

$$\frac{1}{h_1}\frac{\partial(\bar{\rho}\bar{U})}{\partial x^1} + \frac{\partial(\bar{\rho}\bar{W})}{\partial x^3} = 0, \tag{4}$$

$$\frac{\bar{\rho}\bar{U}}{h_1}\frac{\partial\bar{U}}{\partial x^1} + \bar{\rho}\bar{W}\frac{\partial\bar{U}}{\partial x^3} = -\frac{1}{h_1}\frac{d\bar{P}_e}{dx^1} + \frac{1}{Re}\frac{\partial}{\partial x^3}\left(\bar{\mu}\frac{\partial\bar{U}}{\partial x^3}\right), \tag{5}$$

$$\frac{\bar{\rho}\bar{U}}{h_1}\frac{\partial\bar{V}}{\partial x^1} + \bar{\rho}\bar{W}\frac{\partial\bar{V}}{\partial x^3} = \frac{1}{Re}\frac{\partial}{\partial x^3}\left(\bar{\mu}\frac{\partial\bar{V}}{\partial x^3}\right), \tag{6}$$

$$\bar{c}_p \frac{\bar{\rho}\bar{U}}{h_1}\frac{\partial \bar{T}}{\partial x^1} + \bar{c}_p \bar{\rho}\bar{W}\frac{\partial \bar{T}}{\partial x^3} = \frac{1}{Re\,Pr}\frac{\partial}{\partial x^3}\left(\bar{\kappa}\frac{\partial \bar{T}}{\partial x^3}\right) + (\gamma-1)\left\{\frac{\bar{U}M^2}{h_1}\frac{d\bar{P}_e}{dx^1} + \frac{\bar{\mu}M^2}{Re}\left[\left(\frac{\partial \bar{U}}{\partial x^3}\right)^2 + \left(\frac{\partial \bar{V}}{\partial x^3}\right)^2\right]\right\}. \quad (7)$$

Under the boundary layer assumptions, the pressure is constant in the direction normal to the boundary layer, i. e. $\bar{P} = \bar{P}_e(x^1)$. The equation of state can then be expressed as $\gamma M^2 \bar{P}_e = \bar{\rho}\bar{T}$, and the streamwise derivative of the pressure is given as

$$\frac{d\bar{P}_e}{dx^1} = -\bar{\rho}_e \bar{U}_e \frac{d\bar{U}_e}{dx^1}.$$

For a given pressure distribution given by the pressure coefficient

$$C_p = \frac{p - p_\infty}{\frac{1}{2} r_\infty \bar{q}_\infty^2},$$

the values at the boundary layer edge are given as

$$\bar{P}_e = \frac{\bar{P}_e}{\bar{P}_\infty}\frac{1}{\gamma M^2}, \quad \bar{T}_e = \left(\frac{\bar{P}_e}{\bar{P}_\infty}\right)^{\frac{\gamma-1}{\gamma}}, \quad \bar{\rho}_e = \left(\frac{\bar{P}_e}{\bar{P}_\infty}\right)^{\frac{1}{\gamma}},$$

$\bar{U}_e = \sqrt{\bar{Q}_e^2 - \bar{V}_e^2}$, and $\bar{V}_e = \sin\psi$, where

$$\frac{\bar{P}_e}{\bar{P}_\infty} = \frac{p_e}{p_\infty} = 1 + \frac{1}{2}C_p \gamma M^2, \quad \bar{Q}_e^2 = 1 + \frac{1 - \bar{T}_e \bar{c}_{p\infty}}{(\gamma-1)\frac{1}{2}M^2}.$$

Here, we have used the assumptions that for an inviscid, steady, and adiabatic flow the total enthalpy is constant along a streamline, and the isentropic relations are used to obtain the relation between total and static quantities. A domain Ω_B is defined for equations (4)–(7) such that $x^1 \in [X_S, X_1]$, $x^2 \in [Z_0, Z_1]$ and $x^3 \in [0, \infty)$. The no-slip condition is used for the velocity components and the adiabatic wall condition for the temperature. In the free stream, the streamwise and spanwise velocity components, and the temperature takes the corresponding values at the boundary layer edge. This can be written as

$$\left[\bar{U}, \bar{V}, \bar{W}, \frac{\partial \bar{T}}{\partial x^3}\right](x^1, 0) = [0,0,0,0] \qquad \forall x^1 \in [X_S, X_1],$$
$$\lim_{x^3 \to +\infty} \left[\bar{U}, \bar{V}, \bar{T}\right](x^1, x^3) = \left[\bar{U}_e, \bar{V}_e, \bar{T}_e\right](x^1) \;\; \forall x^1 \in [X_S, X_1].$$

Equations (4)–(7) are integrated in the downstream direction normal to the leading edge with an initial condition given by the solution at the stagnation line. In the following sections we denote the solution of the boundary layer state $\bar{\mathbf{Q}} = (\bar{U}, \bar{V}, \bar{W}, \bar{T})$ in order to simplify the presentation.

2.2.2 Disturbance equations

The disturbances analyzed here are assumed to be time- and spanwise periodic waves as

$$\widetilde{\mathbf{Q}}(x^1, x^2, x^3, t) = \hat{\mathbf{Q}}(x^1, x^3)\Theta(x^1, x^2, t), \tag{8}$$

where

$$\Theta(x^1, x^2, t) = \exp \imath \left(\int_{X_0}^{x^1} \alpha(x')\, dx' + \beta x^2 - \omega t \right).$$

Disturbances are superimposed on the mean flow at a streamwise position denoted X_0. We assume a scale separation Re^{-1} between the weak variation in the x^1-direction and the strong variation in the x^3-direction. Further, it is assumed that $\partial/\partial x^1 \sim O(Re^{-1})$ and $W \sim O(Re^{-1})$. Introducing the ansatz (8) and the assumptions above in the linearized governing equations, keeping terms up to order $O(Re^{-1})$, yields a set of nearly parabolic partial differential equations, see Bertolotti *et al.* [7], Malik & Balakumar [18], Simen [28] and Herbert [14]. The system of equations, called Parabolized Stability Equations (PSE), are lengthy and therefore written here as

$$\mathcal{A}\hat{\mathbf{Q}} + \mathcal{B}\frac{\partial \hat{\mathbf{Q}}}{\partial x^3} + \mathcal{C}\frac{\partial^2 \hat{\mathbf{Q}}}{(\partial x^3)^2} + \mathcal{D}\frac{1}{h_1}\frac{\partial \hat{\mathbf{Q}}}{\partial x^1} = \mathbf{0}, \tag{9}$$

where $\hat{Q} = \left[\hat{\rho}, \hat{U}, \hat{V}, \hat{W}, \hat{T}\right]^T$. The coefficients of the 5×5 matrices $\mathcal{A}, \mathcal{B}, \mathcal{C}$ and $\mathcal{D}$ are found in Pralits *et al.* [24]. A domain Ω_P for equation (9) is defined such that $x^1 \in [X_0, X_1]$, $x^2 \in [Z_0, Z_1]$ and $x^3 \in [0, \infty)$. The boundary conditions corresponding to equation (9) are given as

$$\left[\hat{U}, \hat{V}, \hat{W}, \hat{T}\right](x^1, 0) = [0, 0, 0, 0] \qquad \forall x^1 \in [X_0, X_1],$$
$$\lim_{x^3 \to +\infty} \left[\hat{U}, \hat{V}, \hat{W}, \hat{T}\right](x^1, x^3) = [0, 0, 0, 0] \quad \forall x^1 \in [X_0, X_1],$$

To remove the ambiguity of having x^1-dependence of both the amplitude and wave function in the ansatz, and to maintain a slow streamwise variation of the amplitude function $\hat{\mathbf{Q}}$, a so called 'auxiliary condition' is introduced

$$\int_0^{+\infty} \hat{\mathbf{Q}}^H \frac{\partial \hat{\mathbf{Q}}}{\partial x^1}\, dx^3 = 0. \tag{10}$$

Equation (9) is integrated in the downstream direction normal to the leading edge with an initial condition given by local stability theory. At each x^1-position the streamwise wavenumber α is iterated such that the condition given by equation (10) is satisfied. After a converged streamwise wavenumber has been obtained, the growth rate based on the disturbance kinetic energy is calculated from the relation

$$\sigma = -\alpha_i + \frac{\partial}{\partial x^1}(\ln \sqrt{\hat{E}}),$$

where

$$\hat{E} = \int_0^{+\infty} \bar{\rho}\, (|\hat{U}|^2 + |\hat{V}|^2 + |\hat{W}|^2)\, dx^3.$$

The growth rate can then be used to predict the transition location using the so called e^N-method, see van Ingen [32], Smith & Gamberoni [29] and Arnal [4]. The N-factor based on the disturbance kinetic energy of a single disturbance is given as

$$N_E = \int_{X_{n1}}^{X} \sigma \, dx^1.$$

A complete description of equation (9) is found in Pralits *et al.* [24], and the numerical schemes used here are given in Hanifi *et al.* [13].

2.3 Formulation of a problem of NLF design

The measure of the kinetic energy, as the streamwise integral over a defined domain, of several different disturbances, with respective maximum growth rate at different positions, has been successfully applied in an optimal control problem using mean flow suction as control variable, see Pralits & Hanifi [25]. The size of K disturbances superimposed on the mean flow at an upstream position X_0, is measured by their total kinetic energy as

$$E_K = \frac{1}{2} \sum_{k=1}^{K} \int_{X_{ms}}^{X_{me}} \int_{Z_0}^{Z_1} \int_{0}^{+\infty} \widetilde{\mathbf{Q}}_k^H M \widetilde{\mathbf{Q}}_k \, h_1 \, dx^1 \, dx^2 \, dx^3. \tag{11}$$

Here X_{ms} and X_{me} are the first and last streamwise positions between which the disturbance kinetic energy is integrated, and adds the possibility to evaluate E_K in a streamwise domain within $[X_0, X_1]$.

The designed objective function J_C should simultaneously delay the transition, reduce the pressure drag, and, in addition, penalize changes in the coefficients of lift, and pitch-moment:

$$\begin{aligned} J_C = {} & \lambda_U E_1 + \lambda_D C_D \\ & + \frac{1}{2}\lambda_L \left(C_L - C_L^0\right)^2 + \frac{1}{2}\lambda_M \left(C_M - C_M^0\right)^2 , \end{aligned} \tag{12}$$

where the drag, lift and pitch moment coefficients are calculated from the inviscid flow only as

$$\begin{aligned} C_D &= \sum_{i \,\in\, \mathcal{V}(\partial\Omega_w)} \frac{p_i \mathbf{n}_i \cdot \mathbf{d}_D}{\frac{1}{2}\rho_\infty \mathbf{v}_\infty^2 S_{\text{ref}}}, \\ C_L &= \sum_{i \,\in\, \mathcal{V}(\partial\Omega_w)} \frac{p_i \mathbf{n}_i \cdot \mathbf{d}_L}{\frac{1}{2}\rho_\infty \mathbf{v}_\infty^2 S_{\text{ref}}}, \\ C_M &= \sum_{i \,\in\, \mathcal{V}(\partial\Omega_w)} \frac{p_i \mathbf{d}_M \cdot \left(\mathbf{x}_i - \mathbf{O}_{\text{ref.}}\right) \times \mathbf{n}_i}{\frac{1}{2}\rho_\infty \mathbf{v}_\infty^2 S_{\text{ref}} L_{\text{ref}}}. \end{aligned} \tag{13}$$

were $\mathbf{d}_D$ is a unit vector in the direction of the farfield velocity, $\mathbf{d}_D = -\mathbf{v}_\infty / |\mathbf{v}_\infty^2|$, $\mathbf{d}_L$ is a unit vector orthogonal to $\mathbf{d}_D$ and, $\mathbf{d}_M$ is a unit vector orthogonal to $\mathbf{d}_D$ and $\mathbf{d}_L$.

Constraints are further imposed on the feasible designs in order to produce smooth shapes and to enforce geometric constraints. These are constant cross-sectional area, fixed trailing edge

and a fixed region of the airfoil around the leading edge. The last is applied to a region between 0 of the chord length and X_{ms} (0.043) and is meant to eliminate variations in the location of the stagnation point, which, in the current state of development of our codes, could not be accounted for in the sensitivity of the propagation of the disturbances.

2.4 Gradient calculation

It is shown in [2] that the adjoint approach enables an efficient computation of the gradient of the energy E_K (11) with respect to the shape. Observing that we avoided any real coupling between the equations, which would occur if we accounted for the boundary layer displacements on the inviscid flow, the adjoint equations are also solved sequentially (first the adjoint PSE, then the adjoint BLE, and finally the adjoint Euler). However, the adjoint of the BLE and Euler equations, respectively, have forcing terms that depend on the solution of the adjoint PSE and BLE equations, respectively. The adjoint of the PSE equations is, as it is usual, forced by a partial derivative of the energy of the disturbance. The final expression of the shape gradient also depends explicitly on the solutions of the three adjoint equations.

The gradient of J_C (12) is a linear combination of the gradients of E_1, C_D, C_L and C_M. We refer to Amoignon [1] for the calculation of the gradients of the drag, lift and pitch moment coefficients using the discrete adjoint of the Euler equations.

The solution of the adjoint equations and additional post-processing, involving for example the mesh movement algorithm, gives the gradient of J with respect to the normal displacements of the nodes on the airfoil (see next section) ∇J_y.

3 Parameterization

The position of the nodes that discretize the shape is determined here given normal displacements of all nodes on the airfoil with respect to the initial discretization (mesh) $\mathbf{y} \in \mathbb{R}^n$. A parameterization of the displacements ($\mathbf{y}$) enables to define feasible designs, that is to impose geometric constraints as well as some smoothness of the shape.

Smooth shapes are obtained, together with (linear) geometric constraints, by forcing the vectors of displacements $\mathbf{y}$ to be solution of a quadratic programming problem (QP), see Amoignon [1], of the form

$$\mathbf{y} = \arg \left\{ \begin{array}{l} \min\limits_{\mathbf{v} \in \mathbb{R}^n} \dfrac{1}{2} \mathbf{v}^T \mathrm{A}_s \mathbf{v} - \mathbf{v}^T \mathrm{M}_s \mathbf{a}, \\ \mathrm{C}^T \mathbf{v} = \mathbf{b} \end{array} \right. , \tag{14}$$

where A_s is the stiffness matrix associated with the Laplace operator on Γ (the surface of the airfoil), M_s is a mass matrix, $\mathrm{C} \in \mathbb{R}^{n \times m}$ is a matrix whose columns are the gradients of constraints (m) imposed on the displacements and $\mathbf{b}$ is the vector of values imposed to the constraints (in $\mathbb{R}^m$). In the case without geometric constraints ($m = 0$ in (14)) the solution to (14) is solution of the discretized Poisson problem defined by

$$\mathrm{A}_s \tilde{\mathbf{y}} = \mathrm{M}_s \mathbf{a} \, . \tag{15}$$

Adding constraints ($m \geq 1$ in (14)) means that the solution of (14) fulfils exactly the relations

$$\mathrm{C}^T \mathbf{y} = \mathbf{b} \, , \tag{16}$$

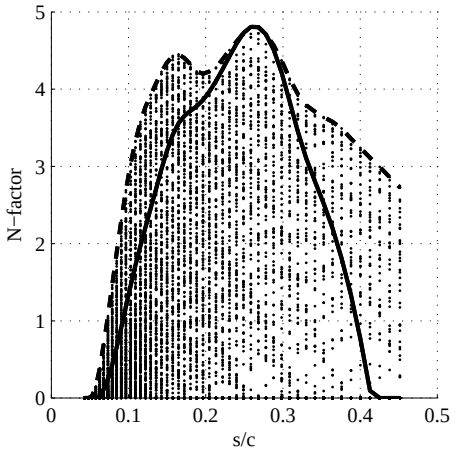

Figure 1: N-factor values for 165 modes (dots) at initial design with dimensional frequency $f = [5, 20]$ kHz ($\Delta f = 1$ kHz), spanwise wavenumber $\beta = [0, 2500]$ $1/m$ ($\Delta\beta = 2501/m$). The mode used in the optimization (solid) is the one having the largest maximum value. The envelope of envelopes (EoE) (dash) gives a picture of the growth of all studied modes.

and, according to some norm $\mathbf{y}$ is the closest to the solution of the discretized Poisson problem. It is a known result of optimization theory [22] that the solution $\mathbf{y}$ of the QP (14) is obtained by solving the Karush-Kuhn-Tucker (KKT) system

$$\begin{pmatrix} \mathrm{A}_s & -\mathrm{C} \\ -\mathrm{C}^T & 0 \end{pmatrix} \begin{pmatrix} \mathbf{y} \\ \lambda \end{pmatrix} = \begin{pmatrix} \mathrm{M}_s\mathbf{a} \\ -\mathbf{b} \end{pmatrix}, \tag{17}$$

where $\lambda \in \mathbb{R}^m$ is a vector of Lagrange multipliers. The system (17) is the first order optimality conditions for the problem (14).

Such a parameterization implies that the controls are the vector $\mathbf{a}$, right side of equation (15), and the vector $\mathbf{b}$, right side of the constraints relations (16). From the gradient with respect to the displacements ∇J_y the gradient with respect to $\{\mathbf{a}, \mathbf{b}\}$, the variables of design in our method, is obtained by solving an adjoint problem, see Amoignon [1], of the form

$$\begin{pmatrix} A_s^T & -C \\ -C^T & 0 \end{pmatrix} \begin{pmatrix} \mathbf{y}^* \\ \lambda^* \end{pmatrix} = \begin{pmatrix} \nabla J_y \\ \mathbf{0} \end{pmatrix}, \tag{18}$$

from which it holds that

$$\nabla J_a = M_s^T \mathbf{y}^* \quad \text{and} \quad \nabla J_b = -\lambda^*. \tag{19}$$

4 Results

The RAE-2822 airfoil is optimized at transonic flow conditions, $M_\infty = 0.734$, $\alpha = 2.1875$ ($C_L^0 = 0.84$), $Re_\infty = 6.5 \times 10^6$ (9600 meters ASL) by minimizing J_C (12). The optimization algorithm concists of a quasi-Newton method (BFGS) with a cubic line search, [22].

A stability analysis of a large number of modes with different frequencies f, and spanwise wave numbers β corresponding to different wave angles, is performed prior to the optimization, on the original design. The wave angle is defined as the angle between the wave number vector

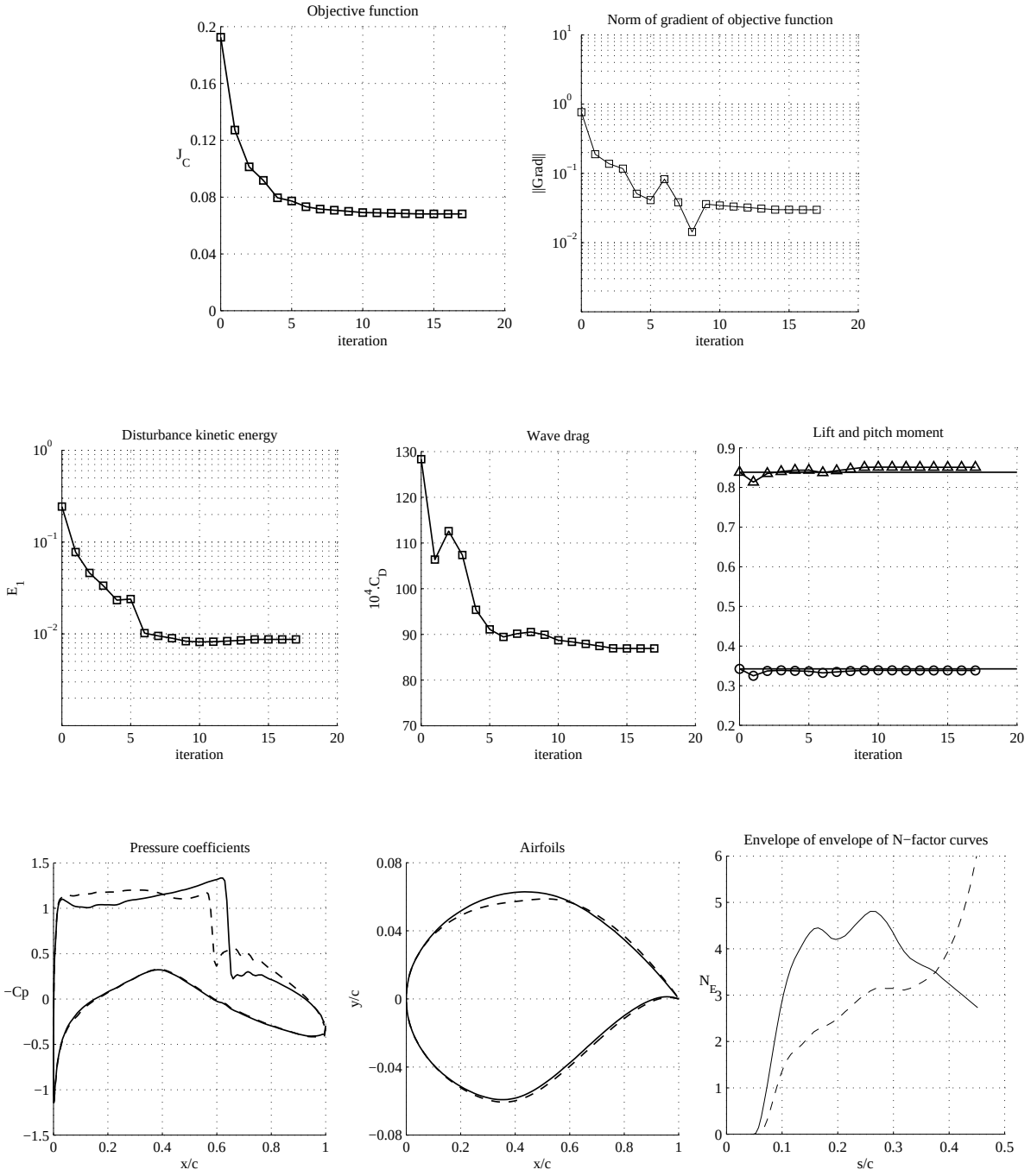

Figure 2: Top left: Objective function, top right: norm of gradient. Centre left: disturbance kinetic energy, centre centre: wave drag, centre right: lift (triangle-solid) and pitch moment (circle-solid) coefficients, initial design (solid). Bottom left: pressure coefficient, bottom centre: shape, bottom right: envelope of envelopes of N-factor curves. Comparison between initial (solid) and final design (dash).

k and the inviscid streamline. The corresponding N-factors are calculated from these results, and the optimization uses the mode which has the largest N-factor value with respect to all other modes, see fig. 1. The reason of this particular choice is that it has been shown in previous studies on optimal control, see Pralits *et al.* [26] and Pralits & Hanifi [25], that a control that successfully decreases the amplification of the above disturbance also have a damping effect on other instability waves of the same type. It is common in transition prediction, to compute the envelope or envelopes (EoE) of the N-factor curves (i. e. envelope over both frequency and spanwise wave number). Transition is then assumed to occur at the position where the EoE curve first attains an empirically determined value. This curve also serves as a measure of the efficiency of a control or design, computed by minimizing a single disturbance, on a large number of disturbances. The choice of spanwise wave number corresponds to wave angles between zero and 85 degrees. Results are presented in fig. 2. The wave drag experiences an increase during one optimization step while the deviation of lift and pitch moment coefficients are forced closer to their respective initial values. The position at which the maximum value of the EoE curve occurs for the final design is placed downstream of the initial one.

5 Conclusions

The present results show that gradient-based Natural Laminar Flow (NLF) design can efficiently be performed combining the solutions of the adjoint equations of the Euler, boundary layer and stability equations.

The work presented here is an ongoing project and current efforts are made to include additional physical modelling, for example to account for the occurence of separated flows.

As no iterative coupling exist between the pressure distribution and the thickness of the boundary layer, this constitutes an approximation. This can be overcomed replacing the inviscid flow analysis with a RANS analysis. This development should include the adjoint of the RANS equations.

REFERENCES

[1] O. Amoignon. Adjoint-based aerodynamic shape optimization, 2003. IT Licentiate theses 2003-012, Department of Information Technology, Division of Scientific Computing, Uppsala University, Box 337, SE-751 05 Uppsala, Sweden.

[2] O. Amoignon, Jan O. Pralits, A Hanifi, M. Berggren, and D.S. Henningson. Shape optimization for delay of laminar-turbulent transition. Technical Report FOI−R−−0919−−SE, Swedish Defence Research Agency, FOI, Aeronautics Division, FFA, SE-172 90 Stockholm, Sweden, 2003.

[3] W.K. Anderson and D.L. Bonhaus. Airfoil design on unstructured grids for turbulent flows. *AIAA Journal*, 37(2):185–191, 1999.

[4] D. Arnal. Boundary layer transition: Predictions based on linear theory. Special course on 'progress in transition modeling', March-April 1993, AGARD-R-793, 1993. 2-1–2-63.

[5] T.J. Barth. Aspects of unstructured grids and finite-volume solvers for the Euler and Navier–Stokes equations. In *Special Course on Unstructured Methods for Advection Dominated Flows*, pages 6–1–6–61. AGARD Report 787, May 1991.

[6] O. Baysal and K. Ghayour. Continuous adjoint sensitivities for optimization with general cost functionals on unstructured meshes. *AIAA Journal*, 39(1):48–55, 2001.

[7] F. P. Bertolotti, Th. Herbert, and S.P. Spalart. Linear and nonlinear stability of the Blasius boundary layer. *J. Fluid Mech.*, 242:441–474, 1992.

[8] G.W. Burgreen, O. Baysal, and M.E. Eleshaky. Improving the efficiency of aerodynamic shape optimization. *AIAA Journal*, 32(1):69–76, 1994.

[9] P. Eliasson. Edge, a Navier–Stokes solver, for unstructured grids. Technical Report FOI-R–0298–SE, Swedish Defence Research Agency, Stockholm, November 2001.

[10] J. Elliot. *Aerodynamic based on the Euler and Navier–Stokes equations using unstructured grids*. PhD thesis, MIT Dept. of Aero. and Astro., 1998.

[11] O. Enoksson. Shape optimization in compressible inviscid flow. Licenciate Thesis LiU-TEK-LIC-2000:31, 2000. Institute of Technology, Linkpings University, Dept. of Math.

[12] B. E. Green and J. L. Whitesides. A method for the constrained design of natural laminar flow airfoils. *AIAA Paper*, (96-2502), 1996.

[13] A. Hanifi, D. S. Henningson, S. Hein, and M. Bertolotti, F. P.and Simen. Linear non-local instability analysis - the linear NOLOT code. *FFA TN*, 1994-54, 1994.

[14] Th. Herbert. Parabolized stability equations. *Annu. Rev. Fluid Mech.*, 29:245–283, 1997.

[15] A. Jameson. Optimum aerodynamic design using CFD and control theory. *AIAA Paper*, (95-1729), 1995.

[16] A. Jameson, N.A. Pierce, and L. Martinelly. Optimum aerodynamic design using the Navier-Stokes equations. *AIAA Paper*, (97-0101), 1997.

[17] R.D. Joslin. Overview of laminar flow control. Technical Report 1998-208705, NASA, Langley Research Center, Hampton, Virginia, Oct 1998.

[18] M. R. Malik and P. Balakumar. Nonparallel stability of rotating disk flow using PSE. In M.Y. Hussaini, A. Kumar, and C.L. Streett, editors, *Instability, Transition and Turbulence*, pages 168–180. Springer, 1992.

[19] V. M. Manning and I. M. Kroo. Multidisciplinary optimization of a natural laminar flow supersonic aircraft. *AIAA Paper*, (99-3102), 1999.

[20] B. Mohammadi. A new optimal shape procedure for inviscid and viscous turbulent flows. *Int. J. Numer. Meth. Fluids*, 25:183–203, 1997.

[21] M. Nemec and D.W. Zingg. Towards efficient aerodynamic shape optimization based on the Navier–Stokes equations. *AIAA Paper*, (2001-2532), 2001.

[22] J. Nocedal and S. Wright. *Numerical Optimization.* Springer Series in Operations Research, 1999.

[23] J. O. Pralits. Towards optimal design of vehicles with low drag: Applications to sensitivity analysis and optimal control. Licentiate thesis KTH/MEK/TR-01/07, Kungl Tekniska Högskolan, SE-100 44 Stockholm, 2001.

[24] J. O. Pralits, C. Airiau, A. Hanifi, and D. S. Henningson. Sensitivity analysis using adjoint parabolized stability equations for compressible flows. *Flow, Turbulence and Combustion*, 65(3/4):321–346, 2000.

[25] J. O. Pralits and A. Hanifi. Optimization of steady suction for disturbance control on infinite swept wings. *Phys. Fluids*, 15(9):2756–2772, 2003.

[26] J. O. Pralits, A. Hanifi, and D. S. Henningson. Adjoint-based optimization of steady suction for disturbance control in incompressible flows. *J. Fluid Mech.*, 467:129–161, 2002.

[27] J. J. Reuther, A. Jameson, J. J. Alonso, M. J. Rimlinger, and D. Saunders. Constrained multipoint aerodynamic shape optimization using an adjoint formulation and parallel computers, part 1. *J. Aircraft*, 36(1):51–60, 1999.

[28] M. Simen. Local and non-local stability theory of spatially varying flows. In M. Hussaini, A. Kumar, and C. Streett, editors, *Instability, Transition and Turbulence*, pages 181–201. Springer, 1992.

[29] A. M. O. Smith and N. Gamberoni. Transition, pressure gradient and stability theory. Technical Report ES 26388, Douglas Aircraft Co., 1956.

[30] B.I. Soemarwoto. *Multi-Point Aerodynamic Design by Optimization.* PhD thesis, Delft University of Technology, Faculty of Aerospace Engineering, P.O. Box 5058, 2600 GB Delft, Netherlands, 1996.

[31] C. Sung and J.H. Kwon. Accurate aerodynamic sensitivity analysis using adjoint equations. *AIAA Journal*, 38(2):243–250, 2000.

[32] J. L. van Ingen. A suggested semiempirical method for the calculation of the boundary layer transition region. Technical Report VTH-74, Department of Aeronautical Engineering, University of Delft, 1956.